Cysteine-Directed Cross-Linking Demonstrates That Helix 3 of SecE Is Close to Helix 2 of SecY and Helix 3 of a Neighboring SecE†

Andreas Kaufmann, Erik H. Manting, Andreas K. J. Veenendaal, Arnold J. M. Driessen,* and Chris van der Does

Department of Microbiology and Groningen Biomolecular Sciences and Biotechnology Institute, University of Groningen, Kerklaan 30, 9751 NN Haren, The Netherlands

Received March 8, 1999; Revised Manuscript Received May 10, 1999

ABSTRACT: Preprotein translocation in *Escherichia coli* is mediated by translocase, a multimeric membrane protein complex with SecA as the peripheral ATPase and SecYEG as the translocation pore. Unique cysteines were introduced into transmembrane segment (TMS) 2 of SecY and TMS 3 of SecE to probe possible sites of interaction between the integral membrane subunits. The SecY and SecE single-Cys mutants were cloned individually and in pairs into a *secYEG* expression vector and functionally overexpressed. Oxidation of the single-Cys pairs revealed periodic contacts between SecY and SecE that are confined to a specific α-helical face of TMS 2 and 3, respectively. A Cys at the opposite α-helical face of TMS 3 of SecE was found to interact with a neighboring SecE molecule. Formation of this SecE dimer did not affect the high-affinity binding of SecA to SecYEG and ATP hydrolysis, but blocked preprotein translocation and thus uncouples the SecA ATPase activity from translocation. Conditions that prevent membrane deinsertion of SecA markedly stimulated the interhelical contact between the SecE molecules. The latter demonstrates a SecA-mediated modulation of the protein translocation channel that is sensed by SecE.

In the well-studied general secretory pathway of *Escherichia coli*, preproteins are targeted to the cytoplasmic membrane either as ribosome-bound nascent chains by a signal recognition particle and FtsY (*1*, *2*) or as completely synthesized polypeptides. Proteins which are secreted through the post-translational pathway can be kept translocation competent by the export-dedicated molecular chaperone SecB (*3*, *4*). Both targeting routes converge at a membrane protein complex termed translocase (*5*). Translocase consists of a peripherally membrane-associated ATPase, SecA (*6*), and the SecYEG heterotrimeric integral membrane protein complex (*7*). The dimeric SecA is activated for SecB recognition when bound to the membrane at SecYEG (*4*, *8*). SecB donates the preprotein to SecA, and is released into the cytosol upon the exchange of SecA-bound ADP[1] for ATP (*9*). The latter reaction elicits a conformational change that permits SecA domains to insert into the membrane with the concomitant insertion of the preprotein (*10*). The inserted preprotein is released from its association with SecA upon hydrolysis of ATP (*11*), and SecA reverts to its membrane surface-bound state. SecA may rebind the partially translocated preprotein, and complete translocation may occur via multiple cycles of ATP binding and hydrolysis (*11*−*13*). In the absence of SecA association, translocation may also be driven by the proton motive force (*11*, *14*).

The translocase holoenzyme is formed by only SecA, SecY, and SecE (*15*, *16*). However, SecG copurifies with the SecYE complex (*7*, *17*), and its presence markedly enhances the efficiency of in vitro preprotein translocation (*18*). SecD, SecF, and YajC are integral membrane proteins that assemble into a complex that interacts with SecYEG (*16*). They may add to the fidelity of the translocation reaction as overexpression of the SecDFYajC complex stabilizes SecA in the membrane-inserted state (*19*, *20*). SecD and SecF are not essential for preprotein translocation, but in their absence, cells are no longer able to sustain a proton motive force and are cold sensitive for growth (*21*, *22*). In vitro experiments have demonstrated that the SecYEG complex suffices to support efficient SecA-dependent preprotein translocation (*7*, *17*, *23*).

The SecYEG complex shares functional and structural characteristics with the Sec61p protein-conducting channel of the eukaryotic endoplasmic reticulum (*24*, *25*). High-resolution electron microscopy images of the mammalian and yeast Sec61p complex show ring-like oligomeric structures, which are formed after interaction with the ribosome (*26*, *27*). These structures seem to consist of two to four Sec61p trimers with a central pore. Recently, it has been shown that the bacterial SecYE of *Bacillus subtilis* exhibits quasi-pentagonal structures, which resemble the Sec61p system (*28*). These structures are thought to consist of an oligomeric assembly of three SecYE subunits.

Both biochemical and genetic data have demonstrated that SecY and SecE interact, but the exact sites of interaction

† These investigations were supported by a PIONIER grant of The Netherlands Organization for Scientific Research (NWO), by the Life Sciences Foundation (SLW), and by the Council for Chemical Sciences of The Netherlands Organization for Scientific Research (CW-NWO).

* To whom correspondence should be addressed. E-mail: a.j.m.driessen@biol.rug.nl. Telephone: (50) 3632164. Fax: (50) 3632154.

[1] Abbreviations: AMP-PNP, adenosine 5′-(β,γ-imidotriphosphate); ADP, adenosine 5′-diphosphate; ATP, adenosine 5′-triphosphate; CBB, Coomassie brilliant blue; DTT, dithiothreitol; IMVs, inner membrane vesicles; IPTG, isopropyl β-D-thiogalactopyranoside; pAb, polyclonal antibody; SDS−PAGE, sodium dodecyl sulfate−polyacrylamide gel electrophoresis; TMS, transmembrane segment.

10.1021/bi990539d CCC: $18.00 © 1999 American Chemical Society
Published on Web 06/18/1999

Table 1: Plasmids Used in This Study[a]

plasmid	relevant characteristics	mutations	ref
pET349	N-terminally His-tagged SecYEG		*17*
pET608	PET610 with SecY(C385S)	C385S (TGC → AGC)	this study
pET609	PET610 with SecY(C329C)	C329S (TGT → AGT)	this study
pET607	Cys-less SecYEG in pET610		this study
pET610	pET349 with Δ*Hin*cII in *secE*	L60C (CTG → CTC)	this study
pET626	SecE(S105C) in pET607	S105C (TCA → TGT)/Δ*Cla*I (ATCGAT → ATCGAC)	this study
pET627	SecE(L106C) in pET607	L106C (CTG → TGT)/Δ*Cla*I (ATCGAT → ATCGAC)	this study
pET628	SecE(I107C) in pET607	I107C (ATC → TGC)/Δ*Cla*I (ATCGAT → ATCGAC)	this study
pET629	SecE(L108C) in pET607	L108C (CTG → TGT)/Δ*Cla*I (ATCGAT → ATCGAC)	this study
pET630	SecE(W109C) in pET607	W109C (TGT → TGT)/Δ*Cla*I (ATCGAT → ATCGAC)	this study
pET636	SecY(F78C) in pET607	F78C (TTT → TGT)/Q146Q (CAA → CAG)	this study
PET637	SecY(A79C) in pET607	A79C (GCT → TGT)/Q146Q (CAA → CAG)	this study
PET638	SecY(L80C) in pET607	L80C (CTG → TGT)/Q146Q (CAA → CAG)	this study
PET639	SecY(G81C) in pET607	G81C (GGG → TGT)/Q146Q (CAA → CAG)	this study
PET640	SecY(I82C) in pET607	I82C (ATC → TGC)/Q146Q (CAA → CAG)	this study
pET301	SecE in pET324		this study
pET1602	SecE(S105C) in pET324		this study
pET1603	SecE (L106C) in pET324		this study
pET1604	SecE(I107C) in pET324		this study
pET1605	SecE(L108C) in pET324		this study
pET1606	SecE(W109C) in pET324		this study

[a] Double-Cys mutants are not described in the table. Their names are derived from combinations of the names of the single-Cys mutants. pET636/623, for example, overexpresses SecYEG with the mutations F78C and L107C in SechYn and SecE, respectively.

have not been identified. The synthetic lethality of various combinations of SecY (*prlA*) and SecE (*prlG*) signal sequence suppressor mutants suggests an interaction between the periplasmic loop 1 (P1) of SecY and P2 of SecE, and indicate that transmembrane segment (TMS) 7 and TMS 10 of SecY are close to TMS 3 of SecE (*29*, *30*). Cytoplasmic domain 4 (C4) of SecY has been suggested to interact with C2 of SecE (*31*, *32*). To obtain detailed insight into the molecular architecture of the SecYEG complex, we have carried out cysteine scanning mutagenesis. This is a powerful technique that has been used to reveal the helix packing and structure−function relationships in polytopic membrane proteins (*33*, *34*). On the basis of the interaction between P1 of SecY and P2 of SecE and the observation that TMS 1 and 2 of SecE are not essential for its function (*35*), we have selected TMS 2 of SecY and TMS 3 of SecE to introduce single cysteine residues. By combining single-Cys mutants, we were able to directly demonstrate specific contacts between these TMSs. In addition, a specific helical face of TMS 3 of SecE interacts with a neighboring SecE molecule. The latter interaction is stimulated when SecA membrane deinsertion in the presence of a preprotein is blocked, and suggests an oligomeric structure of the SecYEG complex where at least two SecE subunits are in close proximity.

EXPERIMENTAL PROCEDURES

Materials. E. coli SecA (*6*), SecB (*36*), and proOmpA (*37*) were purified as described previously. ProOmpA was iodinated as described for preAmyL (*38*), and stored frozen in 6 M urea and 50 mM Tris-HCl (pH 7.8). Wild-type and mutant SecYEG complexes were purified as described previously and reconstituted into liposomes of *E. coli* phospholipid by detergent dilution (*17*). Polyclonal antibodies (pAb) raised against purified His-tagged SecY and SecE, and against a synthetic peptide corresponding to a SecG domain, were obtained as described previously (*17*). A stock solution of 80 mM Cu^{2+}(phenanthroline)$_3$ complex was prepared by mixing 120 μL of 0.36 M 1,10-phenanthroline in 50% ethanol with 60 μL of 0.24 M $CuSO_4$.

Bacterial Strains and Growth Conditions. For all experiments, *E. coli* strain SF100 (*39*) was used. Cells were grown aerobically at 37 °C on L-broth in the presence of 100 μg/mL ampicillin in a shaking incubator until the end of the logarithmic phase. For the induction of plasmid-encoded genes under the control of an IPTG inducible promoter, exponentially growing cultures were supplemented with 0.5 mM isopropyl β-D-thiogalactopyranoside (IPTG) at an OD_{660} of 0.6, and growth was continued for an additional 2 h.

Plasmid Construction. The vector pET349 (SechYnEG$^+$) allows the overproduction of His-tagged SecYEG under control of the IPTG-inducible trc promoter (*17*, *40*). To facilitate cloning and the introduction of unique Cys mutations in SecY and SecE, the *Hin*cII site in SecE was removed from pET349, resulting in pET610 (Table 1). To construct a Cys-less SecY, Cys329 and Cys385 were substituted for serine residues in the *secY* gene of pET605, resulting in pET608 and pET609, respectively. These mutations were transferred to pET610, yielding pET607 which expresses the Cys-less SecYEG complex with a His tag at the amino terminus of SecY. pET607 was used to reintroduce single Cys mutations into SecY and SecE. To facilitate the screening for correct mutants, silent modifications in restriction sites were made. Insertion of a single Cys in TMS 3 of SecE was accompanied by the deletion of the *Cla*I site between SecY and SecE (ATCGAT → ATCGAC), and insertion of the single Cys in TMS 2 of SecY was accompanied with the deletion of the *Stu*I site in SecY Q146Q (CAA → CAG). Single-Cys mutants of TMS 2 of SecY were combined with the Cys mutants in TMS 3 of SecE by exchange of the SecYE *Eco*RI−*Bam*HI fragment. Overexpression of single-Cys SecE mutants was achieved by cloning the appropriate *Nco*I−*Bam*HI SecE fragments in pET324. All mutageneses were carried out via two-step PCR, and constructs were confirmed by sequence analysis on a Vistra DNA sequencer 725 using the automated Δtaq sequencing kit (Amersham, Buckinghamshire, U.K.). All other DNA techniques followed standard procedures.

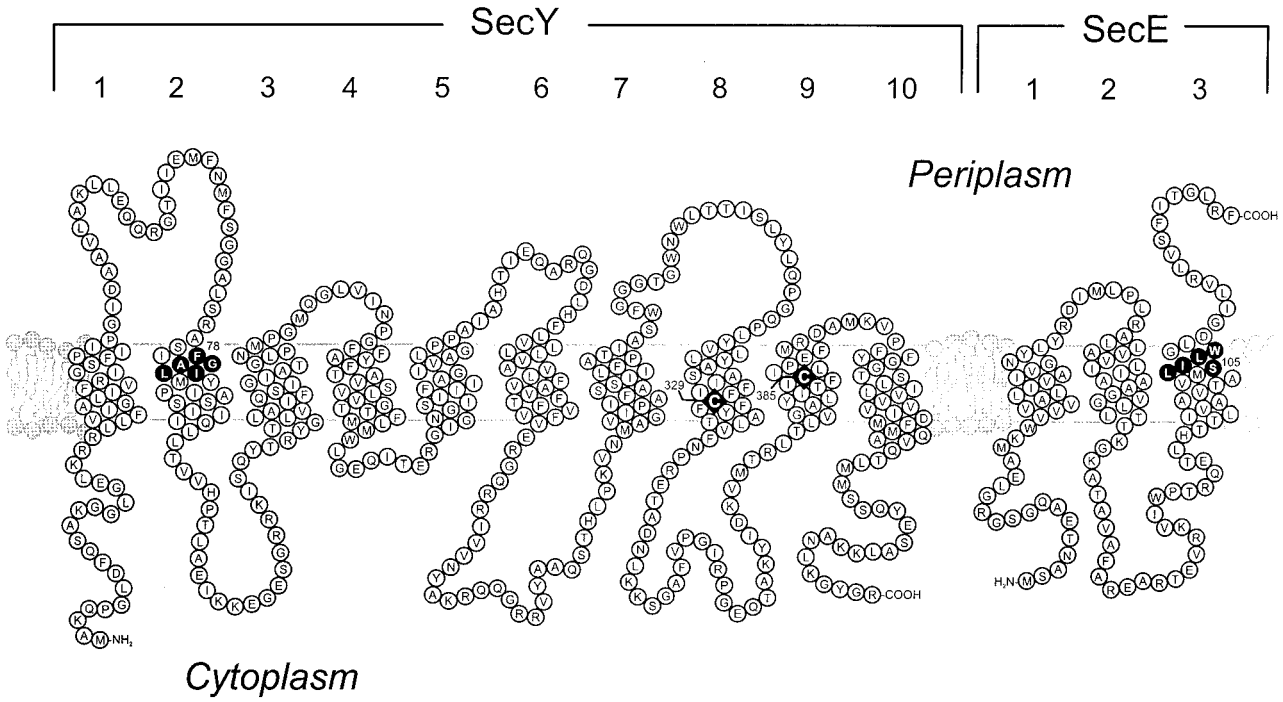

FIGURE 1: Topology model of SecY and SecE. The endogenous cysteine residues that were replaced with serine residues to create the Cys-less SecY are denoted as black diamonds. Single Cys mutations in TMS 2 of SecY and TMS 3 of SecE are denoted as black circles.

Isolation of Inner Membrane Vesicles. A rapid membrane isolation procedure was developed to facilitate the analysis of a large number of mutant SecYEG complexes. Liquid nitrogen-frozen cells were quickly thawed at 37 °C, and diluted with an equal volume of 20% glycerol and 50 mM Tris-HCl (pH 8.0) (buffer A). The suspension was subjected to French press treatment (four times at 8000 psi), diluted with an equal volume of buffer A, and cleared from debris by centrifugation (4000*g* for 10 min). Membranes were collected from the supernatant by centrifugation (40000*g* for 90 min), resuspended in buffer A, and loaded onto a four-step sucrose gradient that consisted of 0.3, 0.9, 0.9, and 0.3 mL of a 36, 45, 51, and 54% (w/v) sucrose solution in 50 mM Tris-HCl (pH 8.0), respectively. Inner membranes vesicles (IMVs) were separated from outer membranes through velocity centrifugation (250 000 rpm for 30 min, Beckmann TLA 100.4 rotor), collected from the gradient, and diluted with 5 volumes of buffer A. Purified IMVs were recollected by centrifugation (40000*g* for 90 min), resuspended in buffer A at a concentration of 10 mg/mL, and stored in liquid nitrogen.

Cross-Linking. For assays of disulfide bridge formation, vesicles were incubated for 30 min on ice in the presence of 1 mM Cu^{2+}(phenanthroline)$_3$ (oxidized) or, as a control, with 10 mM dithiothreitol (DTT) (reduced). Oxidation was terminated with 25 mM neocuproine to protect the unreacted thiols, and the samples were analyzed on 10 or 15% SDS−PAGE, followed by Western blotting and immunostaining with α-SecY, α-SecE, and α-SecG pAbs. The extent of SecE(L106C) cross-linking after preincubation was measured with vesicles that had been reduced with 5 mM DTT before dilution in the translocation reaction mixture. Reaction mixtures were then incubated as indicated, placed on ice, and oxidized with 1 mM Cu^{2+}(phenanthroline)$_3$ as described.

Translocation Assays. Translocation assays were performed in 50 μL of buffer B consisting of 50 mM HEPES/KOH (pH 7.5), 30 mM KCl, 5 mM $Mg(Ac)_2$, and 0.5 mg/mL bovine serum albumin (BSA). Creatine phosphate (10 mM) and creatine kinase (0.5 μg) were added as an ATP-regenerating system. Reaction mixtures furthermore consisted of 1.6 μg of SecB, 1 μg of SecA, 1 μL of ^{125}I-labeled denatured proOmpA [1 mg/mL in 6 M urea and 50 mM Tris-HCl (pH 7.5)], and 10 μg of SecYEG$^+$ IMVs or 6.5 μg of SecYEG proteoliposomes that had been preincubated for 30 min at 0 °C in the presence of 5 mM DTT or 1 mM Cu^{2+}-(phenanthroline)$_3$. Reaction mixtures were energized with 2 mM ATP and kept at 37 °C, and at various time points, samples were taken, chilled on ice, and treated with proteinase K (0.1 mg/mL) for 15 min. Reaction mixtures were then precipitated (20000*g* for 10 min) with ice-cold trichloric acid (10% w/v), washed with acetone, and analyzed by SDS−PAGE on 12% PAA gels. For SecA membrane insertion assays, reactions were performed with 0.2 μg of ^{125}I-labeled SecA and unlabeled proOmpA.

Other Analytical Techniques. Binding assays were performed as described previously (*41*). Translocation ATPase activity of urea-treated IMVs or SecYEG proteoliposomes was measured with proOmpA as the substrate (*42*). SecA membrane insertion assays in which [^{125}I]SecA was used were performed as described previously (*10*). Protein concentrations were determined by the method of Lowry (*43*) in the presence of SDS using BSA as a standard. Semidry Western blotting (Trans-Blot apparatus, Bio-Rad, Hercules, CA) was performed at 4 mA/cm^2 of blotting membrane (PVDF, Boehringer) for 45 min, using a buffer consisting of 48 mM Tris, 30 mM glycine, and 20% (v/v) methanol, with or without 0.1% (w/v) SDS.

RESULTS

Construction and Activity of Single-Cysteine Mutants of SecY and SecE. To investigate the interaction between SecY TMS 2 and SecE TMS 3, we have employed a cysteine

scanning mutagenesis approach. The *E. coli* SecY contains two endogenous cysteines, i.e., Cys329 and Cys385 located in TMS 8 and 9, respectively (Figure 1). SecE and SecG are devoid of Cys residues. A Cys-less SecY was constructed by replacing Cys329 and Cys385 with serine residues using site-directed mutagenesis. The Cys-less SecY was subsequently used to introduce five (F78C, A79C, L80C, G81C, and I82C) unique Cys residues into a consecutive stretch of TMS 2 to cover at least one turn of this putative α-helical segment. Likewise, five (S105C, L106C, I107C, L108C, and W109C) unique Cys residues were introduced into TMS 3 of SecE. These mutations are predicted to be located in the part of the TMS close to the periplasmic face of the membrane (Figure 1; *44*, *45)*. The single-Cys SecY and SecE mutants were cloned either individually or as pairs into the *secYEG* expression vector under control of the *trc* promotor with an amino-terminal His tag on SecY (*40*) (see Table 1). Inner membrane vesicles (IMVs) derived from cells that express the SecYEG complex were checked by SDS−PAGE, CBB staining, and Western blotting using pAbs against SecY, SecE, and SecG. With each of the constructs, SecY, SecE, and SecG were overexpressed to the same extent as the wild-type SecYEG complex. This is shown in Figure 2A for the Cys-less SecYEG and the complexes that bear the single-Cys SecE mutations, but identical results were obtained for the individual SecY mutants, and the SecE−SecY mutant combinations. Since SecY is only stable when overexpressed together with SecE (*46*), it appears that with each of the Cys mutants a stable SecY−SecE interaction is achieved. IMVs were analyzed for the in vitro translocation of ^{125}I-labeled proOmpA (Figure 2B) and for the SecA translocation ATPase activity in the presence of proOmpA (Figure 2C). These assays were performed in the presence of DTT to prevent possible oxidation of the Cys residues. In all cases, the activities of the mutant SecYEG complexes were similar to that of the wild type. IMVs were also tested for the translocation of [^{125}I]Δ8proOmpA, a proOmpA derivative with a defective signal sequence due to the deletion of Ile8. In contrast to IMVs of the *prlA4* strain (*41*) that expresses the PrlA4 SecY at wild-type levels, none of the overexpressed mutants was able to translocate Δ8proOmpA (data not shown). This suggests that the mutagenesis has not yielded any strong *prlA* or *prlG* mutants. In summary, the Cys-less SecYEG, the single-Cys mutants of SecY and SecE, and the pairs of SecY and SecE mutants are normally overexpressed and are functionally active.

TMS 2 of SecY and TMS 3 of SecE Are Interacting Transmembrane Segments. To identify interhelical contacts between SecY and SecE, the membranes containing the SecYEG complex with the pairs of single-Cys mutants of SecY and SecE were oxidized with 1 mM Cu^{2+}(phenanthroline)$_3$. The reaction was then quenched with 10 mM neocuproine, and protein profiles were analyzed by SDS−PAGE in the absence of reducing agents, Western blotting, and immunodetection using pAbs directed against SecY and SecE. Out of a total of 25 Cys pairs, only the combinations of SecY(F78C) with SecE(L108C), SecY(A79C) with SecE(L108C), and SecY(I82C) with SecE(S105C) yielded a slowly migrating protein band after oxidation that reacted with both pAbs directed against SecY and SecE (Figure 3). This putative cross-linked product of SecY and SecE exhibited an apparent molecular mass of 50 kDa on SDS−PAGE, and its formation was reversed by the addition of DTT (data not shown). The cross-linked product was not observed in membranes containing the Cys-less SecYEG (see Figure 4) or single-Cys mutants of SecY or SecE. Modeling of TMS 2 of SecY and TMS 3 of SecE reveals that all detected cross-links are confined to a distinct helical face, and that the interaction reappears after a single turn of both helical segments (Figure 9). The latter periodicity indicates that TMS 2 of SecY and TMS 3 of SecE are indeed α-helical

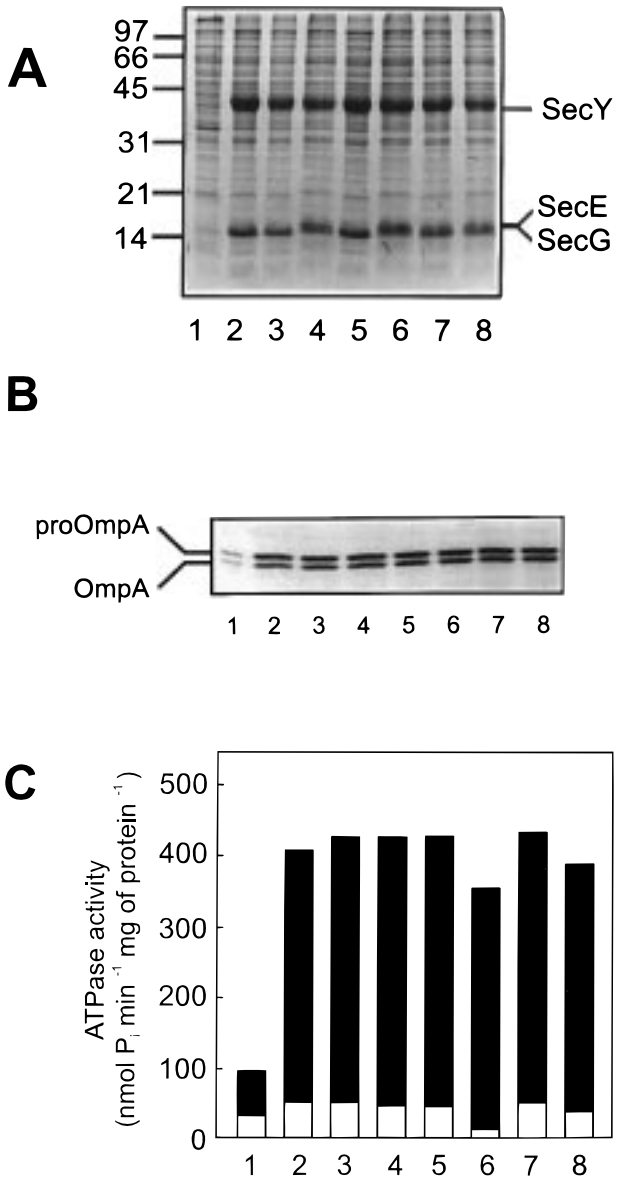

FIGURE 2: Overexpression of SecY, SecE, and SecG proteins in *E. coli* SF100 cells. (A) Coomassie brilliant blue-stained SDS−PAGE of IMVs derived from SF100 cells harboring plasmids pET324 (control, lane 1), pET610 (SecYEG, lane 2), pET607 (Cys-less SecYEG, lane 3), pET626 [SecYE(S105C)G, lane 4], pET627 [SecYE(L106C)G, lane 5], pET628 [SecYE(I107C)G, lane 6], pET629 [SecYE(L108C)G, lane 7], and pET630 [SecYE(W109C)G, lane 8]. The positions of the molecular mass markers are indicated. (B) Translocation of [^{125}I]proOmpA into IMVs. Translocation reactions were performed for 10 min in the presence of SecA and ATP. The positions of proOmpA and OmpA are indicated. Lanes are numbered as described above. (C) SecA ATPase activity of urea-treated IMVs in the absence (white bars) and presence (black bars) of proOmpA. Lanes are numbered as described above.

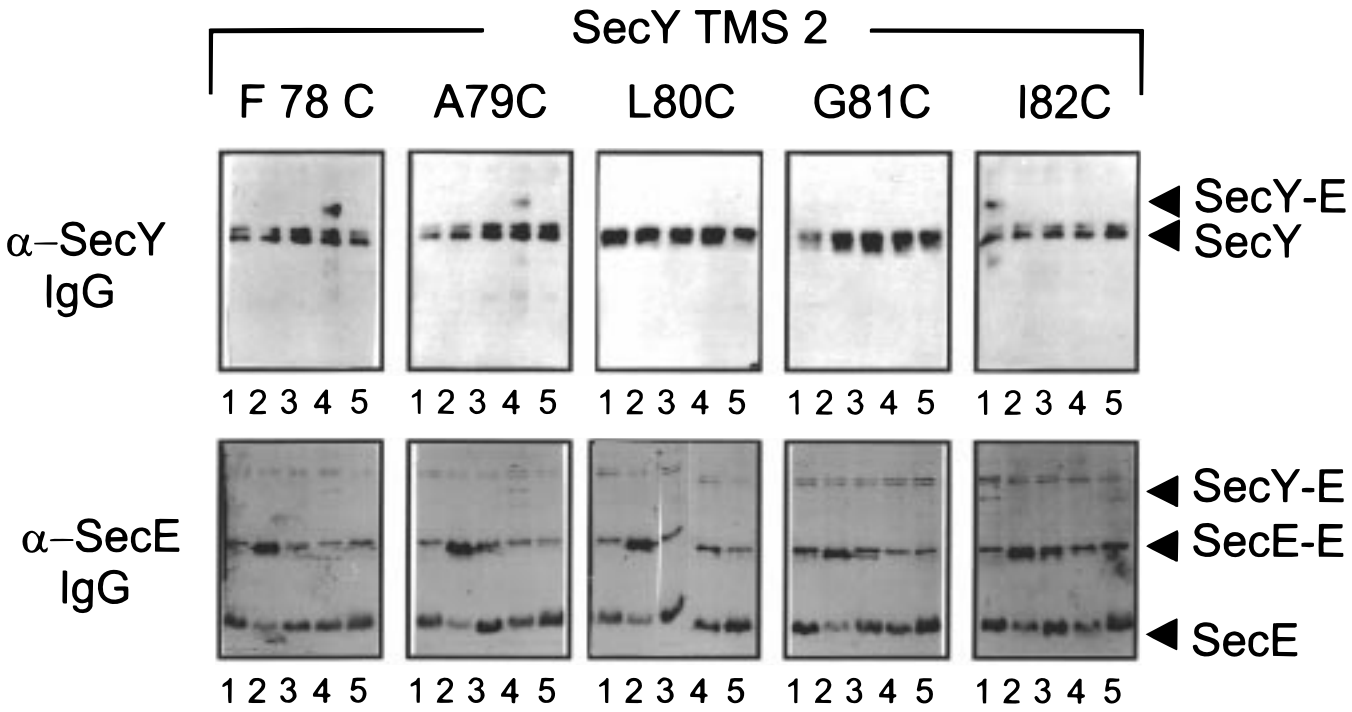

FIGURE 3: Identification of specific cross-links between unique cysteines in TMS 2 of SecY and TMS 3 of SecE. IMVs derived from SF100 cells overexpressing the SecYEG complex containing pairs of the indicated Cys mutants in TMS 2 of amino-terminally His-tagged SecY and the following Cys mutants in TMS 3 of SecE: S105C (lane 1), L106C (lane 2), I107C (lane 3), L108C (lane 4), and W109C (lane 5). IMVs were oxidized for 30 min on ice in the presence of Cu^{2+}(phenanthroline)$_3$, and subsequently quenched with an excess of neocuproine. Samples were analyzed by immunoblotting using pAbs directed against SecY and SecE. Resultant cross-linked products with apparent molecular masses of 50 (SecY−E) and 28 kDa (SecE−E) are denoted. SecY stains as a double band due to the presence of the endogenous SecY, overexpressed His-tagged SecY, and proteolytic loss of the His tag. The protein band that appears in all samples at 30 kDa and slightly above the SecE−E cross-link is outer membrane protein A (OmpA), which is nonspecifically detected by the anti-SecE pAb. Note that this band is not present in the oxidized purified SecYE(L106C)G complexes shown in Figure 4.

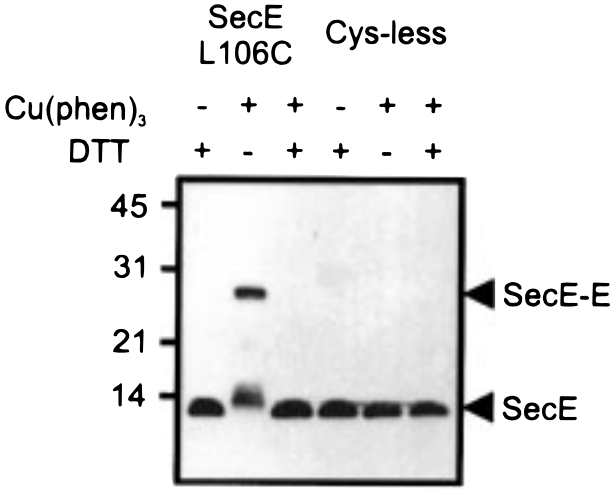

FIGURE 4: The 28 kDa cross-linked product represents a SecE dimer. Proteoliposomes reconstituted with the purified Cys-less SecYEG and SecYE(L106C)G complex (6.5 μg/mL) were oxidized for 30 min on ice in the presence of Cu^{2+}(phenanthroline)$_3$, as indicated, and subsequently quenched with an excess of neocuproine. Samples were separated on SDS−PAGE in the absence or presence of DTT, blotted, and immunostained with pAbs directed against SecE. The position of the 28 kDa cross-linked SecE product is indicated (SecE−E).

and that both TMSs are in close proximity, i.e., within disulfide bonding distance.

SecE(L106C) Contacts a Neighboring SecE Molecule. In all samples that contained the SecE(L106C) mutant, even in combination with the Cys-less SecY, the oxidizing conditions also yielded a highly specific protein band with an apparent molecular mass of 28 kDa (Figure 3). This cross-link stained only with the pAb directed against SecE, and not with the SecY- or SecG-specific antibodies. The 28 kDa cross-linked product disappeared upon incubation with DTT, and was not found with wild-type SecE. On the basis of its size, it may represent an oxidized dimer of SecE(L106C) molecules. To exclude cross-linking of SecE(L106C) with another membrane protein of unknown identity, both the SecYE(L106C)G and Cys-less SecYEG complex were purified to homogeneity (*17*). The SecE(L106C) molecule copurified with SecG and the His-tagged Cys-less SecY with the same stoichiometry as the wild-type SecYEG complex (data not shown), which confirms that the SecE mutant normally interacts with SecY and SecG. Moreover, under oxidizing conditions, the reconstituted SecYE(L106C)G complex again yielded the 28 kDa protein band (Figure 4), while the cross-linked band was not observed with the Cys-less SecYEG complex. This unequivocally demonstrates that oxidation of the SecYE(L106C)G complex results in dimerization of SecE. It is important to stress that the apparent ratio between monomeric SecE and the species cross-linked to SecY or SecE on Western blots depended on the applied blotting conditions. Longer blotting times resulted in a loss of signal of the polypeptide band representing monomeric SecE, whereas shorter blotting times hardly revealed any cross-linked SecE. Therefore, even though the amount of SecE is equal in all samples, the total of immunostained SecE varies. The blotting conditions applied were optimal for visualizing the cross-linked products without complete loss of the monomeric SecE signal. As the unique dimerization

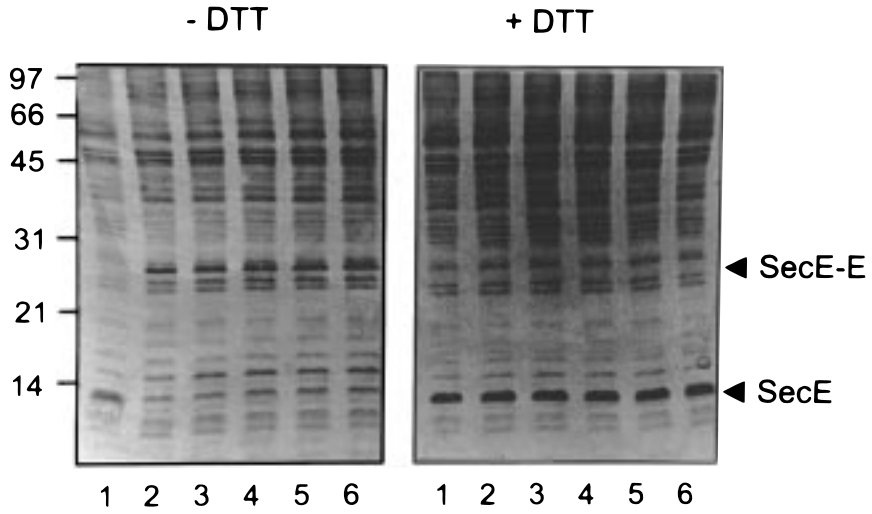

FIGURE 5: Single-Cys mutants of SecE dimerize when overexpressed in the absence of SecY. IMVs derived from SF100 cells overexpressing SecE (wild-type, lane 1), SecE(S105C) (lane 2), SecE(L106C) (lane 3), SecE(I107C) (lane 4), SecE(L108C) (lane 5), and SecE(W109C) (lane 6) were oxidized with Cu^{2+}(phenanthroline)$_3$, quenched with neocuproine, and separated on SDS−PAGE in the absence (−DTT) and presence of DTT (+DTT). Samples were stained with Coomassie brilliant blue, and the position of the SecE dimer is indicated (SecE−E).

of the SecE(L106C) mutant was observed after purification and reconstitution of the SecYE(L106C)G complex, it unlikely results from a loose interaction with SecY or an overstoichiometric expression level of the mutant SecE molecule. The latter is also apparent from the overexpression level of SecE(L106C), which is the same as for the other SecE Cys mutants.

When each of the single Cys SecE mutants was overexpressed separately, i.e., without SecY and SecG, the oxidation-induced formation of the 28 kDa cross-linked product was no longer unique for the SecE(L106C) but occurred with all constructs (Figure 5). Apparently, uncomplexed SecE is in a conformation in which cross-linking of cysteines in TMS 3 readily occurs upon oxidation. However, upon association with SecY, SecE is oriented in such a manner that except for SecE(L106C), all Cys mutants are protected from disulfide bond formation. These results therefore suggest that SecE(L106) cross-links with another SecE molecule within the SecYEG complex (Figure 9) as confirmed by the experiments with the purified SecYEG (Figure 4).

Oxidation of SecYE(L106C)G Inhibits Translocation. To establish whether the formation of the SecE(L106C) dimer had any influence on the activity of the SecYEG complex, Cys-less SecYEG or SecYE(L106C)G was treated with Cu^{2+}-(phenanthroline)$_3$ and analyzed for SecA-dependent proOmpA translocation. These studies were performed with both IMVs (data not shown) and proteoliposomes reconstituted with the purified SecYEG complexes (Figure 6). The level of translocation of proOmpA with SecYE(L106C)G was greatly reduced by oxidation, whereas the Cys-less SecYEG allowed translocation up to a translocation intermediate (I_{31}) with a molecular mass of 31 kDa. The latter is due to the presence of a disulfide bridge in the carboxyl terminus of proOmpA that prevents further translocation (*11*). In IMVs, this intermediate exhibits an apparent molecular mass of 29 kDa due to the removal of the signal peptide by leader peptidase. Upon addition of DTT, proOmpA translocation with Cys-less SecYEG and SecYE(L106C)G occurred at equally effective levels (Figure 6). These results demonstrate that the oxidation-induced dimerization of SecE(L106C)

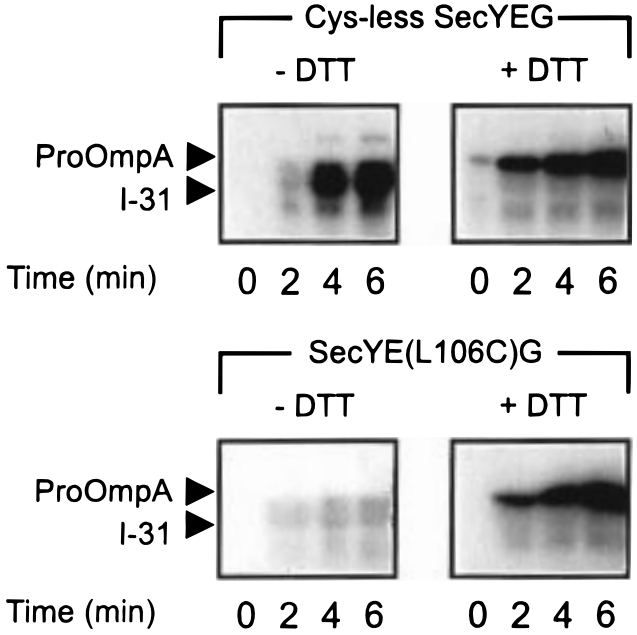

FIGURE 6: Proteoliposomes bearing SecYE(L106C)G are reversibly inactivated upon oxidation. Samples containing Cys-less SecYEG or SecYE(L106C)G proteoliposomes (6.5 μg/mL) were oxidized for 30 min on ice with 1 mM Cu^{2+}(phenanthroline)$_3$, transferred to an environment with a temperature of 37 °C, and further incubated for 5 min in the absence or presence of 10 mM DTT. Translocation was followed in time after the addition of [^{125}I]-proOmpA, SecA (10 μg/mL), and ATP (2 mM). The arrows denote the positions of proOmpA and the translocation intermediate I_{31}.

inactivates translocase in a reversible manner. The effect of oxidation of the SecY−SecE single-cysteine pairs was not further analyzed due to the low efficiency of disulfide bond formation.

Dimerized SecE(L106C) Uncouples the SecA ATPase Activity. The effect of the oxidation of the SecY-bound SecE-(L106C) was further examined by assessing the SecA membrane binding and insertion, and the SecA translocation ATPase activity. SecA binds with high affinity to the SecYEG complex, and with low affinity to the membrane lipids. The binding of ^{125}I-labeled SecA to urea-treated IMVs

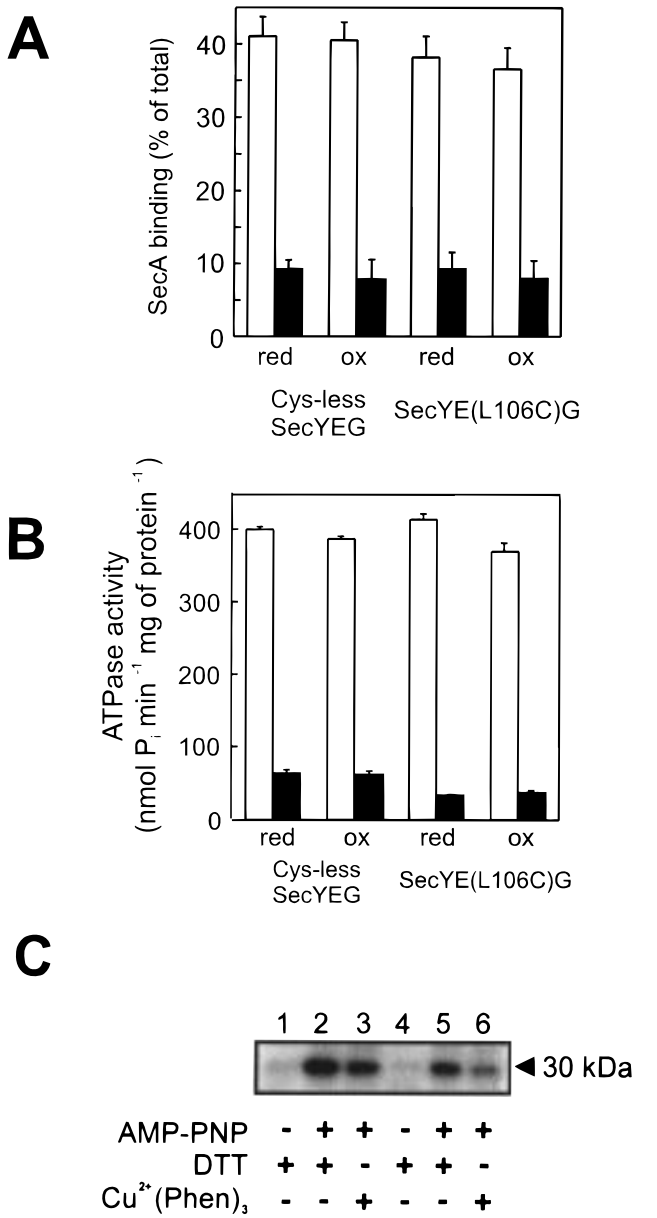

FIGURE 7: Dimerized SecE(L106C) binds SecA with high affinity and does not inhibit membrane insertion, but uncouples the translocation ATPase activity (A) SecA binding. Reduced or oxidized IMVs (50 μg/mL) bearing overexpressed SecYE(L106C)G or Cys-less SecYEG were incubated for 15 min on ice in the presence of 30 nM ^{125}I-labeled SecA. The extent of binding of SecA to the vesicles was determined after their isolation through a 0.2 M sucrose cushion (white bars). The nonspecific binding level was determined in the presence of 500 nM unlabeled SecA (black bars). Error bars represent the mean standard error of three independent experiments. (B) SecA ATPase activity in the presence (white bars) or absence (black bars) of proOmpA. Averages and deviations of two experiments are shown. (C) SecA membrane insertion. The extent of the AMP-PNP-induced membrane insertion of SecA was measured as the level of formation of a 30 kDa ^{125}I-labeled proteolytic SecA fragment in the presence of reduced (+DTT) or oxidized [+Cu^{2+}(phenanthroline)$_3$] IMVs bearing overproduced Cys-less SecYEG (lanes 1−3) or SecYE(L106C)G (lanes 4−6).

that harbor overexpressed Cys-less SecYEG or SecYE(L106C)G was not affected by the oxidation with Cu^{2+}(phenanthroline)$_3$, but was effectively eliminated after the addition of an excess of unlabeled SecA (Figure 7A). This demonstrates that the dimerization of the SecY-bound SecE does not interfere with the number of high-affinity SecA binding sites. Next, we determined whether the SecYEG- and precursor-stimulated SecA ATPase activity was influenced by the oxidation of SecE(L106C). Surprisingly, the amount of ATP hydrolysis by SecA in the presence of proOmpA was identical to that observed with the Cys-less SecYEG complex (Figure 7B). Since the oxidation of the SecE(L106C) results in a near to complete block of translocation, the SecA translocation ATPase appears to be uncoupled from translocation. Membrane insertion of SecA was analyzed by the formation of a protease-protected ^{125}I-labeled 30 kDa fragment upon interaction with the nonhydrolyzable ATP analogue AMP-PNP in the presence of urea-treated IMVs bearing Cys-less SecYEG or SecYE(L016C)G (Figure 7C). Under reducing conditions, both the Cys-less SecYEG and SecYE(L106C)G complex allowed formation of the proteolytic 30 kDa SecA fragment. Oxidizing conditions strongly, but not completely, inhibited 30 kDa formation with the SecYE(L106C)G complex. These data demonstrate that SecA retains the ability to bind with high affinity to the oxidized SecYE(L106C)G complex and to hydrolyze ATP. Since membrane insertion is not completely prevented under oxidizing conditions, it cannot be excluded whether the remaining membrane insertion activity relates to incomplete oxidation of SecE(L106C) or residual activity of the oxidized SecYE(L106C)G channel. We conclude, however, that the oxidized SecYE(L106C)G channel must be in a close-to-functional state to allow SecA binding and an uncoupled translocation ATPase activity.

SecA Modulates the Intrahelical Contact between Neighboring SecE Molecules. To examine whether the formation of the Sec(L106C) dimer was modulated by translocation conditions, conditions that abolished dimer formation were explored. When urea-treated membrane vesicles bearing SecYE(L106C)G were extensively prereduced with 5 mM DTT, diluted in buffer without DTT, and subsequently oxidized by the addition of Cu^{2+}(phenanthroline)$_3$, only a low level of SecE(L106C) dimer was formed (Figure 8, lane 2). We used this method of prereduction as an assay to determine conditions that modulate the efficiency of dimer formation, and in this manner to detect dynamic changes in the subunit interactions of SecYEG during translocation. The yield of dimer formation was not affected by the addition of SecA irrespective of the presence or absence of proOmpA (lanes 4 and 3, respectively) or by the subsequent addition of ATP (lane 5). However, a dramatic elevation of the level of SecE dimer formation occurred when instead of ATP, the nonhydrolyzable ATP analogue AMP-PNP was added to the solution (lane 6). This phenomenon strictly depended on the presence of the preprotein, since in the absence of proOmpA, no stimulation of dimer formation was observed (lane 7). We then tested whether other conditions leading to the stable insertion of SecA had an effect on the SecE(L106C) cross-linking. Indeed, a preprotein-dependent stimulation was observed when ATP-γ-S was used as a nonhydrolyzable ATP analogue (lanes 8 and 9). Nonhydrolyzable ATP analogues block translocation in its initial stage, leading to the processing of the signal sequence by leader peptidase (*11*) and a stabilization of the SecA membrane-inserted state (*10*). To block SecA in its membrane-inserted state during later stages of the translocation reaction, the ATPase inhibitor azide was added 25 min after the addition of ATP (lane 11). Azide interferes with the SecA ATPase activity (*47*), but

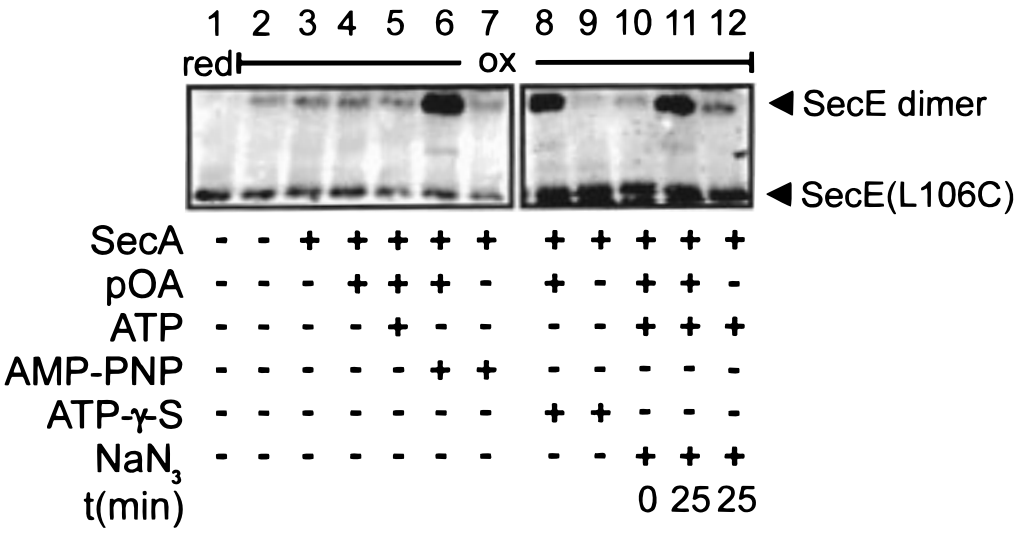

FIGURE 8: Stable membrane insertion of SecA promotes interhelical SecE(L106C) contacts. IMVs containing overproduced SecYE(L106C)G were prereduced with 5 mM DTT and diluted into translocation mixtures containing SecA, proOmpA (pOA), 2 mM ATP, AMP-PNP, or ATPγS, as indicated. NaN_3 (20 mM) was added either before the onset of the translocation reaction (lane 10) or after translocation for 25 min (lanes 11 and 12). After 30 min, samples (lanes 2−12) were oxidized by further incubation for 30 min on ice in the presence of 1 mM Cu^{2+}(phenanthroline)$_3$. Lane 1 corresponds to the reduced control.

enforces the formation of membrane-inserted SecA by preventing its deinsertion (*41*). This effect appears to be strongest during an ongoing translocation reaction (lane 11), as the addition of azide before initiation of translocation with ATP did not result in an increased level of SecE(L106C) dimerization (lane 10). Also in the case of the azide-induced SecA membrane insertion, the effect on the SecE cross-linking was dependent on the presence of preprotein (lane 12). Under the same set of conditions, we were unable to detect a change in the yield of the SecY−SecE cross-link using the SecY(A79C) and SecE(L108C) mutant pair (data not shown). Furthermore, none of the other SecE Cys mutants exhibited dimer formation under the conditions described above. These results demonstrate that translocase undergoes dynamic changes that influence the proximity of two SecY-bound SecE molecules. This phenomenon is coupled to the membrane insertion of SecA and takes place only with active translocase, i.e., in the presence of preprotein.

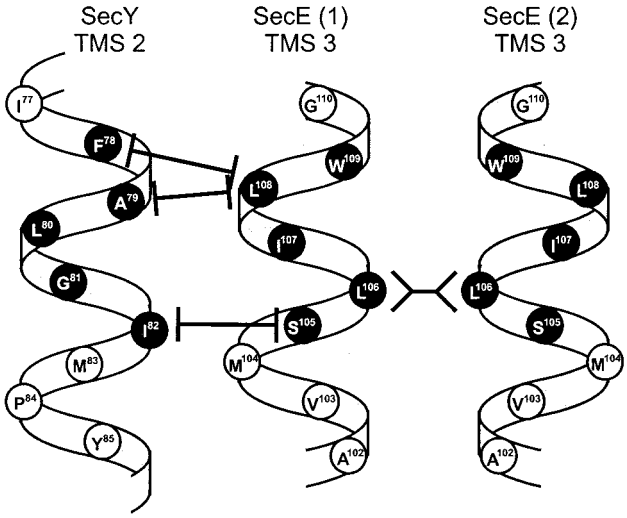

FIGURE 9: Schematic representation showing the periodic sites of interaction between TMS 2 of SecY and TMS 3 of SecE, and the identified site of interaction between TMS 3 of neighboring SecE molecules. In black are denoted the mutagenized amino acids residues that are part of the amino acid sequences of residues 77−85 and 102−110 of SecY and SecE, respectively. For simplicity, the SecY interaction for the second SecE molecule is not shown.

DISCUSSION

In this paper, we provide direct evidence for an interaction between TMS 2 of SecY and TMS 3 of SecE of *E. coli*, and demonstrate that the SecYG-bound SecE interacts with a neighboring SecE molecule. SecA influences the latter interaction in a preprotein- and nucleotide-dependent manner. For this study, we have used a Cys-less SecYEG complex to allow cysteine scanning mutagenesis. The two endogenous Cys residues of SecY were replaced with serine residues, yielding a fully functional SecYEG complex that was subsequently used to introduce unique Cys residues into TMS 2 of SecY (F78−I82) and TMS 3 of SecE (S105−W109). These helical regions were chosen on the basis of the genetically identified interaction between periplasmic loop 1 (P1) of SecY and P2 of SecE (*30*). All mutants could be functionally overexpressed, implying that the SecY−SecE interaction in these mutants is retained as the stability of SecY in the cell is dependent on its interaction with SecE (*46*). None of the cysteine mutants exhibited a strong *prl* phenotype, as evidenced by the inability of these highly overexpressed mutants to translocate Δ8proOmpA, despite the fact that one of the mutated residues SecE(L108) was previously shown to yield a *prlG* suppressor phenotype when substituted for an arginine (*35*).

By means of Cu^{2+}(phenanthroline)$_3$-induced disulfide bond formation, an interaction could be demonstrated between cysteines replacing F78 and A79 in TMS 2 of SecY and L108 in TMS 3 of SecE. These residues are restricted to a specific helical face of both TMSs, and strikingly, cross-linking reappeared when the Cys mutations were moved a single α-helical turn, replacing I82 in SecY and S105 in SecE (Figure 9). L108 in TMS 3 of SecE was found to make disulfide bonds with two adjacent positions in TMS 2 of SecY, suggesting some conformational flexibility in this region or in the side chains of the introduced Cys residues.

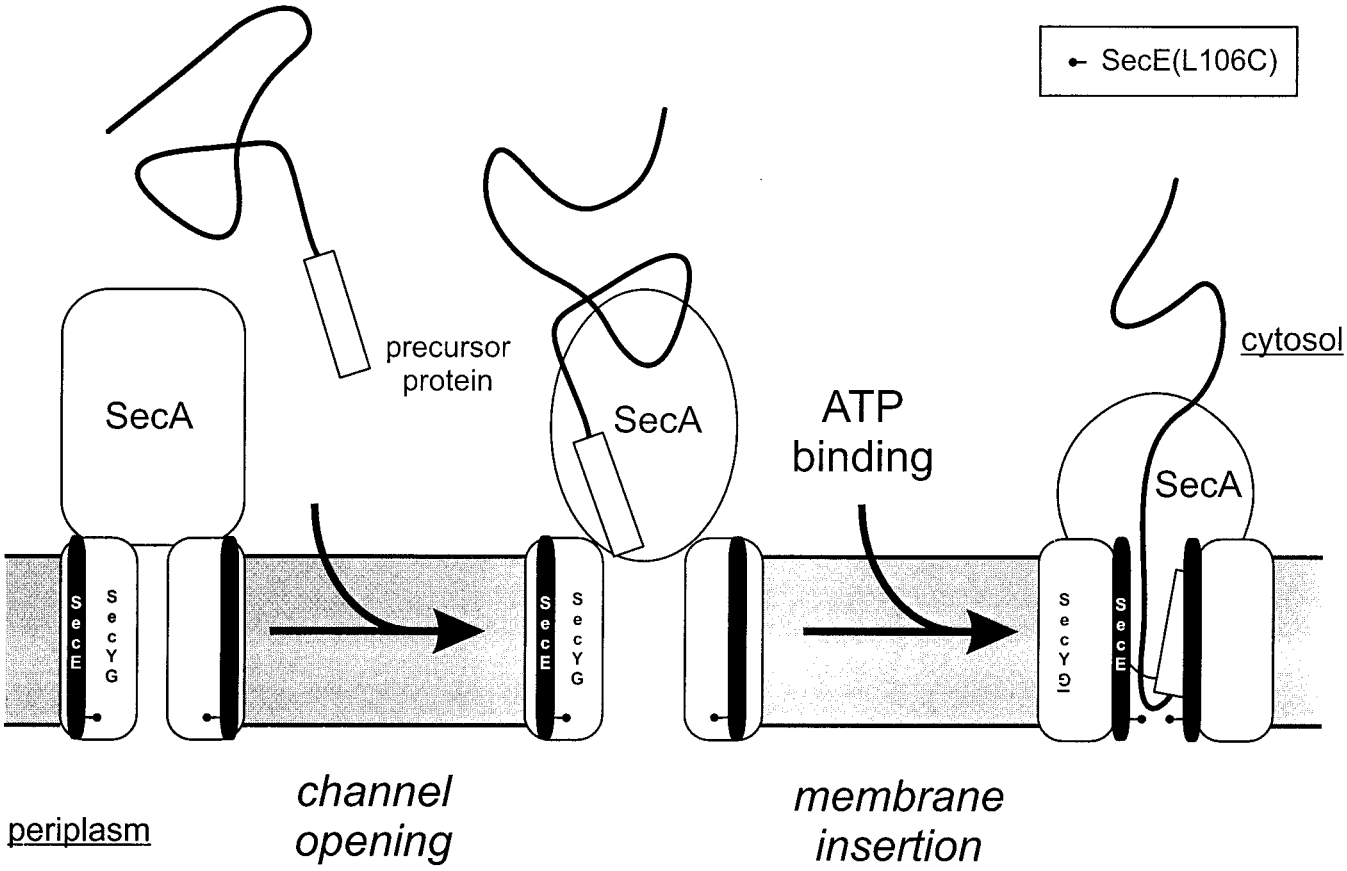

FIGURE 10: Schematic model for the modulation of the SecYEG translocation channel by the membrane insertion of SecA. Binding of a precursor protein activates the SecYEG-bound SecA, which triggers channel opening of an oligomeric assembly of SecYEG complexes. Subsequent binding of ATP to SecA drives the insertion of a SecA domain together with the signal sequence and amino-terminal mature region of the precursor protein into the translocation channel. This process is accompanied by the inversion of the SecG membrane topology (indicated by the reversed G) and a rearrangement of the SecY-bound SecE bringing the L106C residues (represented by a black stalk) at the periplasmic side of SecE TMS 3 in closer proximity. The latter rearrangement may be necessary to accommodate the inserted preprotein. For simplicity, a dimeric assembly of the SecYEG complex is shown.

Previous genetic evidence suggested an interaction between P1 of SecY and P2 of SecE, and we now show that this interaction reflects a close proximity between at least two of the associated transmembrane helices. Interactions of SecY cytoplasmic loop 4 (C4) together with SecE C2 and of TMS 7 and TMS 10 of SecY together with TMS 3 of SecE have been identified genetically (*30*−*32*). TMS 2, 7, and 10 of SecY are the most conserved, whereas TMS 3 of SecE is the only membrane span that is necessary for the SecE function. Most *prlA* mutations of SecY that allow the translocation of signal sequence defective preproteins are clustered in P2, TMS 7, and TMS 10 of SecY (*29*, *30*). TMS 3 of SecE may therefore be surrounded by the conserved core of the integral membrane domain of the translocase, i.e., TMS 2, TMS 7, and TMS 10 of SecY. On the basis of a systematic cross-linking study of the linking of the signal sequence of a preprotein to the yeast translocase, it has been postulated that the signal sequence and Sss1p−SecE bind to the same or overlapping regions in Sec61p−SecY (*48*). The same study shows that TMS 2 and TMS 7 of Sec61p can be cross-linked to the signal sequence. Our report extends this postulate and demonstrates that TMS 2 of SecY is indeed in close proximity of TMS 3 of SecE, specifying this interaction to defined residues. Conditions that lead to the membrane insertion of the signal sequence or that allow preprotein translocation did, however, not affect the extent of the $Cu^{2+}(phenanthroline)_3$-induced cross-linking of SecY(A79C) to Sec(L108C). These conditions also did not affect the cross-linking between other SecE Cys mutants, excluding the possibility that SecE is expelled from the translocase by the signal sequence. These data thus suggest a stable interaction between SecY and SecE that persists during translocation.

One of the five examined Cys mutants of TMS 3 of SecE, SecE(L106C), exhibits a $Cu^{2+}(phenanthroline)_3$-induced dimerization, irrespective of its combination with the wild-type, Cys-less, or single-Cys mutants of SecY. The other four Cys mutants of SecE exhibited such behavior only when overexpressed in the absence of SecY. SecE(L106C) seems to interact with SecY in a manner that is indistinguishable from that of the wild type, which has been shown not to dissociate from SecY in the membrane (*49*). The stability of the SecY−SecE(L106C) interaction was confirmed by purification of the SecYE(L106C)G complex, which after reconstitution showed the same $Cu^{2+}(phenanthroline)_3$-induced dimerization of SecE. The purified SecYE(L106C)G complex provided unequivocal evidence that the cross-linked SecE product indeed consists of a SecE dimer that is associated with the other translocase subunits. Although the oxidized SecYE(L106C)G channel binds SecA and allows it to undergo cycles of ATP binding and hydrolysis, translocation and SecA membrane insertion are severely impaired. Apparently,

this SecYEG channel is trapped in a partially functional state that no longer is able to meet the requirements that allow complete translocation reaction cycles.

The dynamic nature of the SecYEG channel was visualized by the modulation of SecE(L106C) dimerization by SecA. Membrane-inserted SecA affects the conformation of the SecYEG protein translocation channel in such a manner that it affects the proximity of two SecE TMS 3 helices (see the scheme in Figure 10). This was apparent, as stabilization of the membrane-inserted state of SecA by nonhydrolyzable ATP analogues or azide caused a marked stimulation of the Cu^{2+}(phenanthroline)$_3$-induced dimerization of SecE(L106C). As both SecE molecules are part of the SecYEG complex, this event may reflect conformational changes within an oligomeric organization of multiple SecYEG heterotrimers that together form a translocation channel. Such an oligomeric organization of the protein-conducting channel has been demonstrated by electron microscopy for the homologues eukaryotic Sec61p and the *B. subtilis* SecYE complex. In addition, the oligomeric organization of the SecYEG complex explains the paradigm that SecY and SecE do not dissociate in vivo (*49*) but appear to interact dynamically (*50*). Our experiments are consistent with an oligomeric assembly of the SecYEG complex where two SecE molecules are in close proximity, but do not reveal the exact stoichiometry of such a complex. As the sites of interactions between SecY and SecE are restricted to specific regions of the two molecules (refs *30*−*32* and this study), it is most likely that they interact in a stoichiometric fashion. This is also apparent from their interdependent expression and cellular expression levels (*46*, *51*). We therefore propose that the observed SecE−E interaction takes place between two SecYEG subunits within the oligomeric channel.

The modulation of the SecE(L106C) dimerization by SecA strictly required the presence of proOmpA, although SecA membrane insertion with AMP-PNP is precursor-independent (*10*). We therefore postulate that interrelated but separate events underlie the modulation of the translocation channel by preproteins and SecA. First, signal sequence recognition triggers a conformational change in the SecYEG channel and thereby activates or "opens" the translocation channel (Figure 10, *channel opening*). Such a phenomenon has been postulated for both SecYEG (*52*) and the Sec61p protein-conducting channel (*53*). Whereas the pore size of the Sec61 channel upon interaction with the ribosome is around 2 nm (*26*, *27*), it is opened to 4−6 nm in the presence of ribosome-nascent chain complexes (*54*). In the *E. coli* system, the signal sequence recognition may involve a specific conformational state of SecA that triggers opening of the SecYEG channel. Second, the active protein translocation channel undergoes conformational changes during the translocation reaction that are elicited through cycles of conformational changes that take place in the SecA molecule. Only with the precursor-activated translocation channel does SecA membrane insertion trigger the intimate contact between two SecE(L106C) molecules that causes disulfide bond formation (Figure 10, *membrane insertion*). We propose that SecA membrane insertion results in a subunit rearrangement or a conformational change of the active SecYEG translocation channel that brings the L106C residues in SecE in a position favorable for disulfide bond formation (Figure 10).

The modulation of the cross-linking of SecE(L106C) together with the SecG topology inversion (*55*) and SecA cycling at the cytoplasmic membrane (*10*) demonstrate that translocase is a highly dynamic protein complex, and indicate a strong relationship between the conformation of SecA and that of the SecYEG complex. The identified contacts between TMS 2 of SecY and TMS 3 of SecE (Figure 9) can be incorporated into a model of the molecular architecture of the SecYEG complex that will serve as a starting point for identifying further inter- and intramolecular interactions for obtaining a low-resolution molecular model of the integral membrane domain of the translocase.

ACKNOWLEDGMENT

André Boorsma and John Marissen are thanked for technical assistance.

REFERENCES

1. Valent, Q. A., de Gier, J. W., von Heijne, G., Kendall, D. A., ten Hagen-Jongman, C. M., Oudega, B., and Luirink, J. (1997) *Mol. Microbiol. 25*, 53−64.
2. Powers, T., and Walter, P. (1997) *EMBO J. 16*, 4880−4886.
3. Kumamoto, C. A. (1991) *Mol. Microbiol. 5*, 19−22.
4. Hartl, F. U., Lecker, S., Schiebel, E., Hendrick, J. P., and Wickner, W. (1990) *Cell 63*, 269−279.
5. Valent, Q. A., Scotti, P. A., High, S., de Gier, J. W., von Heijne, G., Lentzen, G., Wintermeyer, W., Oudega, B., and Luirink, J. (1998) *EMBO J. 17*, 2504−2512.
6. Cabelli, R. J., Chen, L., Tai, P. C., and Oliver, D. B. (1988) *Cell 55*, 683−692.
7. Brundage, L., Hendrick, J. P., Schiebel, E., Driessen, A. J. M., and Wickner, W. (1990) *Cell 62*, 649−657.
8. Fekkes, P., van der Does, C., and Driessen, A. J. M. (1997) *EMBO J. 16*, 6105−6113.
9. Fekkes, P., de Wit, J. G., van der Wolk, J. P., Kimsey, H. H., Kumamoto, C. A., and Driessen, A. J. M. (1998) *Mol. Microbiol. 29*, 1179−1190.
10. Economou, A., and Wickner, W. (1994) *Cell 78*, 835−843.
11. Schiebel, E., Driessen, A. J. M., Hartl, F. U., and Wickner, W. (1991) *Cell 64*, 927−939.
12. Uchida, K., Mori, H., and Mizushima, S. (1995) *J. Biol. Chem. 270*, 30862−30868.
13. van der Wolk, J. P., de Wit, J. G., and Driessen, A. J. M. (1997) *EMBO J. 16*, 7297−7304.
14. Driessen, A. J. (1992) *EMBO J. 11*, 847−853.
15. Akimaru, J., Matsuyama, S., Tokuda, H., and Mizushima, S. (1991) *Proc. Natl. Acad. Sci. U.S.A. 88*, 6545−6549.
16. Duong, F., and Wickner, W. (1997) *EMBO J. 16*, 2756−2768.
17. van der Does, C., Manting, E. H., Kaufmann, A., Lutz, M., and Driessen, A. J. M. (1998) *Biochemistry 37*, 201−210.
18. Nishiyama, K., Mizushima, S., and Tokuda, H. (1993) *EMBO J. 12*, 3409−3415.
19. Economou, A., Pogliano, J. A., Beckwith, J., Oliver, D. B., and Wickner, W. (1995) *Cell 83*, 1171−1181.
20. Duong, F., and Wickner, W. (1997) *EMBO J. 16*, 4871−4879.
21. Arkowitz, R. A., and Wickner, W. (1994) *EMBO J. 13*, 954−963.
22. Pogliano, J. A., and Beckwith, J. (1994) *EMBO J. 13*, 554−561.
23. Hanada, M., Nishiyama, K. I., Mizushima, S., and Tokuda, H. (1994) *J. Biol. Chem. 269*, 23625−23631.
24. Hartmann, E., Sommer, T., Prehn, S., Gorlich, D., Jentsch, S., and Rapoport, T. A. (1994) *Nature 367*, 654−657.
25. Pohlschroder, M., Prinz, W. A., Hartmann, E., and Beckwith, J. (1997) *Cell 91*, 563−566.
26. Hanein, D., Matlack, K. E., Jungnickel, B., Plath, K., Kalies, K. U., Miller, K. R., Rapoport, T. A., and Akey, C. W. (1996) *Cell 87*, 721−732.

27. Beckmann, R., Bubeck, D., Grassucci, R., Penczek, P., Verschoor, A., Blobel, G., and Frank, J. (1997) *Science 278*, 2123−2126.
28. Meyer, T. H., Ménétret, J. F., Breitling, R., Miller, K. R., Akey, C. W., and Rapoport, T. A. (1999) *J. Mol. Biol. 285*, 1789−1800.
29. Osborne, R. S., and Silhavy, T. J. (1993) *EMBO J. 12*, 3391−3398.
30. Flower, A. M., Osborne, R. S., and Silhavy, T. J. (1995) *EMBO J. 14*, 884−893.
31. Baba, T., Taura, T., Shimoike, T., Akiyama, Y., Yoshihisa, T., and Ito, K. (1994) *Proc. Natl. Acad. Sci. U.S.A. 91*, 4539−4543.
32. Pohlschroder, M., Murphy, C., and Beckwith, J. (1996) *J. Biol. Chem. 271*, 19908−19914.
33. Wu, J., and Kaback, H. R. (1996) *Proc. Natl. Acad. Sci. U.S.A. 93*, 14498−14502.
34. Frillingos, S., Sahin-Toth, M., Wu, J., and Kaback, H. R. (1998) *FASEB J. 12*, 1281−1299.
35. Schatz, P. J., Bieker, K. L., Ottemann, K. M., Silhavy, T. J., and Beckwith, J. (1991) *EMBO J. 10*, 1749−1757.
36. Weiss, J. B., Ray, P. H., and Bassford, P. J., Jr. (1988) *Proc. Natl. Acad. Sci. U.S.A. 85*, 8978−8982.
37. Crooke, E., Guthrie, B., Lecker, S., Lill, R., and Wickner, W. (1988) *Cell 54*, 1003−1011.
38. van Wely, K. H., Swaving, J., and Driessen, A. J. M. (1998) *Eur. J. Biochem. 255*, 690−697.
39. Baneyx, F., and Georgiou, G. (1990) *J. Bacteriol. 172*, 491−494.
40. van der Does, C., den Blaauwen, T., de Wit, J. G., Manting, E. H., Groot, N. A., Fekkes, P., and Driessen, A. J. M. (1996) *Mol. Microbiol. 22*, 619−629.
41. van der Wolk, J. P., Fekkes, P., Boorsma, A., Huie, J. L., Silhavy, T. J., and Driessen, A. J. M. (1998) *EMBO J. 17*, 3631−3639.
42. Lill, R., Cunningham, K., Brundage, L. A., Ito, K., Oliver, D., and Wickner, W. (1989) *EMBO J. 8*, 961−966.
43. lowry, O. H., Rosebrough, N. J., Farr, A. L., and Randall, R. J. (1951) *J. Biol. Chem. 193*, 265−275.
44. Akiyama, Y., and Ito, K. (1987) *EMBO J. 6*, 3465−3470.
45. Downing, W. L., Sullivan, S. L., Gottesman, M. E., and Dennis, P. P. (1990) *J. Bacteriol. 172*, 1621−1627.
46. Matsuyama, S., Akimaru, J., and Mizushima, S. (1990) *FEBS Lett. 269*, 96−100.
47. Oliver, D. B., Cabelli, R. J., Dolan, K. M., and Jarosik, G. P. (1990) *Proc. Natl. Acad. Sci. U.S.A. 87*, 8227−8231.
48. Plath, K., Mothes, W., Wilkinson, B. M., Stirling, C. J., and Rapoport, T. A. (1998) *Cell 94*, 795−807.
49. Joly, J. C., Leonard, M. R., and Wickner, W. T. (1994) *Proc. Natl. Acad. Sci. U.S.A. 91*, 4703−4707.
50. Bieker-Brady, K., and Silhavy, T. J. (1992) *EMBO J. 11*, 3165−3174.
51. Pogliano, K. J., and Beckwith, J. (1994) *J. Bacteriol. 176*, 804−814.
52. Simon, S. M., and Blobel, G. (1992) *Cell 69*, 677−684.
53. Crowley, K. S., Liao, S., Worrell, V. E., Reinhart, G. D., and Johnson, A. E. (1994) *Cell 78*, 461−471.
54. Hamman, B. D., Hendershot, L. M., and Johnson, A. E. (1998) *Cell 92*, 747−758.
55. Nishiyama, K., Suzuki, T., and Tokuda, H. (1996) *Cell 85*, 71−81.

BI990539D